

Fig.3.6 General flow of the fabrication process.

Photolithography

A layer of positive photoresist (S1805) is spun coated on top of the grown chip. The spin coating condition was as follows: 1st spin 500rpm for 5 sec, 2nd spin 6000rpm for 40 sec. The thickness of the resist spun coated under this condition was found about 0.4 μm . For better adhesion of the resist, adhesion-enhanced substance, the primer was first spun coated under the same condition prior to the photoresist. The resist coated substrate was then subjected to a 90 second pre-baking at 110°C with a hot plate to evaporate moisture and to stabilize the resist. Waveguide pattern is defined onto the resist using hard contact photolithography technique in our mask aligner (Karl Suss MJB3 RB) and exposed resist was developed in NMD-3 solution. Typical exposure time in the mask aligner and developing time in our process were 3.7 seconds and 7 seconds respectively. Follow on, the photoresist was post-baked at 120°C for 15 minutes with an oven to strengthen its resistance against chemical etching.

Table 4.2 Photolithography condition

<i>Parameters</i>	<i>Condition</i>
Photoresist	S1805
Spin	
First step speed/time	500 rpm/5 sec
Second step speed/time	6000 rpm/40 sec
Prebake	110°C, 90 sec
Postbake	120 °C, 15 min
Exposure time	3.7 sec
Developing time	7 sec

Wet etching

Uncovered p⁺-InGaAs and p-InP will be etched to form the designed waveguide structure. The etchants are listed in Table 4.3.

Table 3.3 Etchant and etching condition

<i>Layer</i>	<i>Etchant</i>	<i>Mix Ratio</i>	<i>Etching Temperature</i>	<i>Etching Time</i>	<i>Note</i>
p ⁺ -InGaAs	H ₂ SO ₄ :H ₂ O ₂ :H ₂ O	1:1:5	5°C	30 sec	
p-InP	20% HCl	-	R.T	3-4 min	Dip into the ultrasonic cleaner to get rid of the bubbles

Insulator evaporation

Al₂O₃ layer is used to cover and insulate the etched area. The thickness must not be too thick or the lift-off process will fail. Typical thickness is 150-200 nm. Evaporating process relies on Electron Beam (EB) evaporator (ULVAC). In order to cover both sides of the sidewall, the fabricated substrate must be set tilted about 70 degree to the evaporated metal beam in the first half evaporation process and then -70 degree in the second half process.

Lift-off

Without removing the photoresist after etching and continue the insulator evaporator suddenly, the evaporated materials will be on both the substrate and the patterned photoresist. Cleaning the photoresist will remove the evaporated materials over the photoresist away, leaving the negative self-patterned evaporated materials on the surface of the substrate. The cleaner liquid for the lift-off is usually boiling acetone in an ultrasonic cleaner. The intensity of the ultrasonic wave should not be so strong, otherwise the whole sample will crash.

Metal evaporation for the electrode

Because on the chip, there are many parallel straight waveguides, the electrode between the lines must be separated. In the metal evaporation process of the top electrode, the fabricated substrate must be set tilted to the evaporated metal beam. The waveguide will cause the shadow of the evaporated metal beam behind it, thus build the self-separation of the electrodes of the two waveguides. In fact, the electrode occurs on the top of the passive waveguide will have no connection to the electrode occurring behind it.

To make the ohmic contact electrode on p⁺-InGaAs layer, Ti metal is firstly evaporated, following with Au. The thickness is listed in Table 3.4. Note that the listed thickness of the evaporated metals is the measured one, which is different with that monitored by the ULVAC.

Table 4.4 Thickness of the sputtered layer.

<i>Metal</i>	<i>Rate (nm/sec)</i>	<i>Thickness (nm)</i>
Flat alignment		
Ti	0.5	200
Au	1	300
Al ₂ O ₃	1	250

Lapping and bottom contact evaporation

The thickness of the substrate after finished the top surface structures will be too thick and will be very difficult to be cleaved for the high quality facet. The thickness of the substrate thus will be lapping out for 150 um approximately. Then the bottom electrode will be made by the flat alignment metal evaporation.

Fig.3.7 shows the Scanning Electron Microscope (SEM) images of the cross section view of the fabricated EAM. Clear separation of the right side was observed for both reverse ridge and forward ridge structures. Note that the etching of the InGaAs contact layer and InP cladding layer can also be done by Inductively coupled Plasma (ICP) dry etching. Details are given in Chapter V.

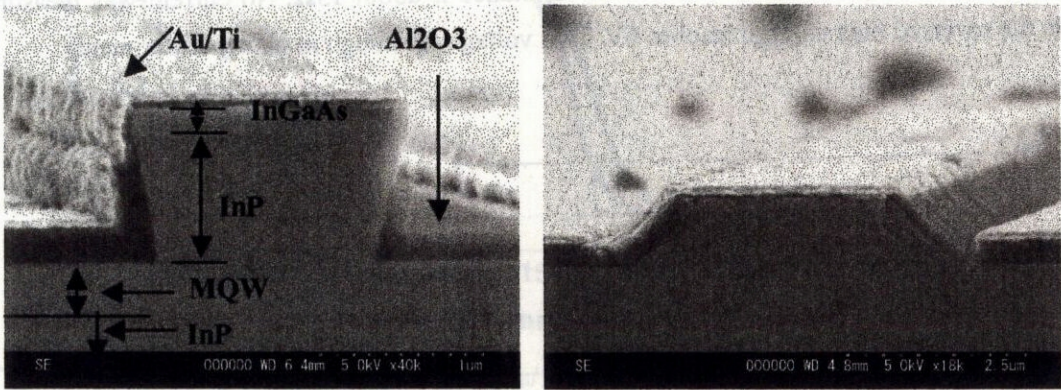


Fig.3.7 Scanning Electron Microscope (SEM) images of the cross section view of the fabricated EAM. (a). Reverse ridge structure. (b) Forward ridge structure.

3.3 Characterization of EAM

All the following measurements are based on sample #3695. The layer stacks are shown in Fig.3.8, and the length of EAM is 270 mm. The MQW consists 10 sets of InGaAlAs/InGaAlAs quantum well, well width = 10 nm, barrier width = 5 nm.

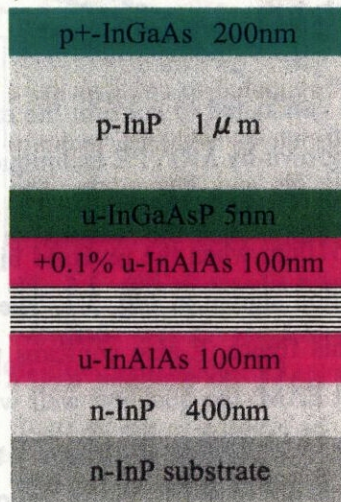


Fig 3.8. Layer structure of the EAM in #3695

3.3.1 I-V

The EAM is composed by a p-i-n diode, and is operated at reversed bias voltages. As the first step, the I-V characteristic is measured.

The threshold voltage is about 1 V and the resistance is about 13Ω . No current was measured while the reversed bias voltage reaches 6V. This voltage is enough in all my experiments.

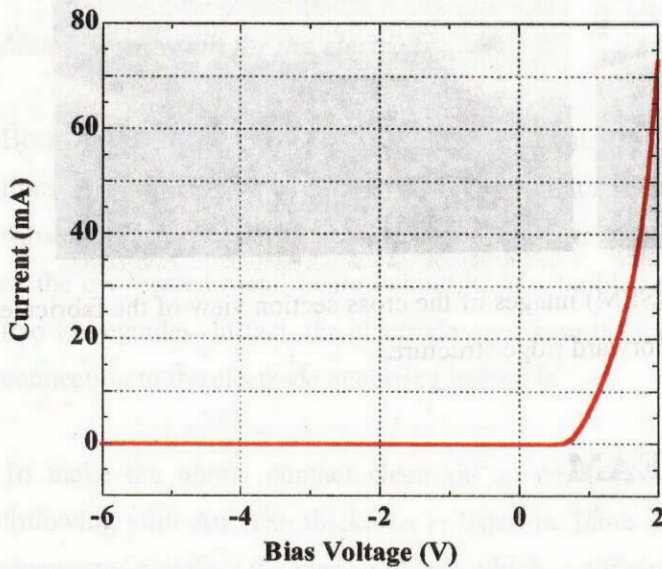


Fig.3.8 I-V characteristics of InGaAlAs/InGaAlAs MQW EAM

3.3.2 Photocurrent spectrum

The photocurrent measurement is conducted to confirm the existence of the excitons and their peak positions of every substrate grown by MOVPE technique. Fig.3.9 shows the photocurrent measurement results for combined TE and TM mode. The wavelength of first the peak is 1490nm, 1495nm, 1500nm and 1510nm when the reversed bias voltage is 0V, 1V, 2V and 4V. They match well with the simulation shown in Fig. 3.3. The TM peak is at around 1450nm. Apparent QCSE is observed in this figure. It also confirms that the grown MQW is of high quality. Note that in the fabricated EAM, the quantum well width is 10nm, while the quantum well width is set to 7 nm. This may be because in the MOVPE growth, the interface between the quantum well and quantum barrier is not so sharp, so the real quantum well is kind of elliptical, not rectangle. So the 7 nm width seems like the effective well width.

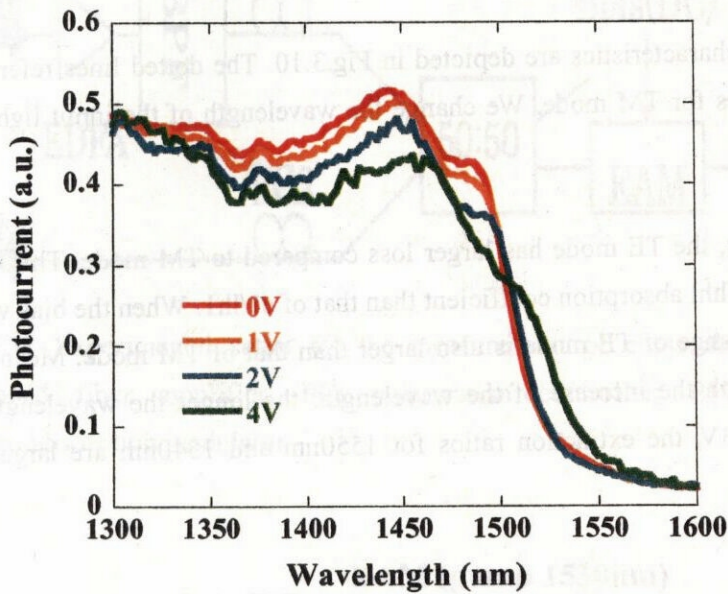


Fig.3.9 Photocurrent spectrum of InGaAlAs/InGaAlAs MQW EAM.

3.3.3 Electrical modulation

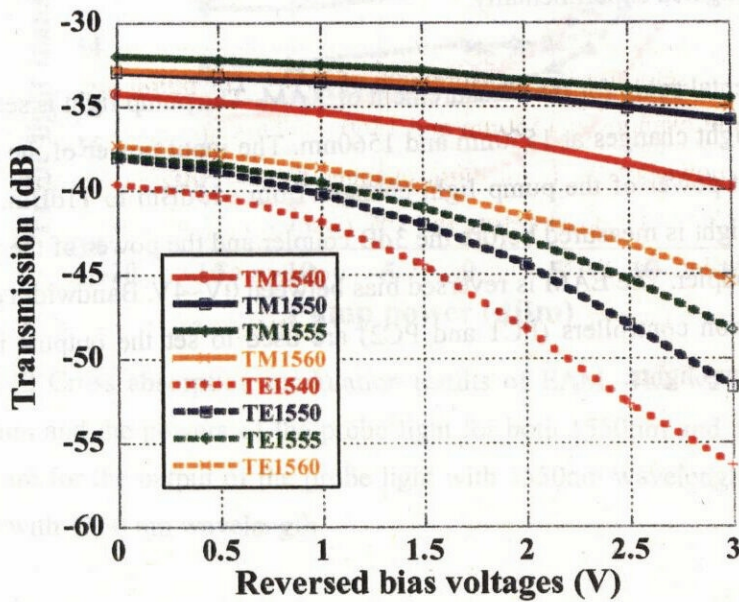


Fig.3.10 Modulation characteristics of MQW EAM. The solid lines denote the TM mode, and dotted lines denote the TE mode

The electrical modulation characteristics are depicted in Fig.3.10. The dotted lines refer to the TE mode and the solid lines for TM mode. We change the wavelength of the input light from 1540nm to 1560nm.

We can see that in all cases, the TE mode has larger loss compared to TM mode. This can be explained by the stronger e_1/h_1 absorption coefficient than that of e_1/h_1 . When the bias voltage increases, the absorption change of TE mode is also larger than that of TM mode. Meanwhile, the absorption decreases with the increase of the wavelength: the longer the wavelength, the weaker the absorption. At 3V, the extinction ratios for 1550nm and 1540nm are larger than 15dB.

3.3.4 Cross absorption modulation (XAM)

The nonlinearity in EAM such as cross absorption modulation (XAM) and cross phase modulation (XPM) is the most concern in my research. Both the novel wavelength converter and all-optical switch are based on these two effects. So at the first step, the nonlinearity in an single EAM should be investigated experimentally.

Fig.3.11 shows the experimental setup for the measurement of XAM. The pump light is set to be at 1530 nm, and the probe light changes at 1550nm and 1560nm. The input power of the probe light is 0dBm, and the input power of the pump light changes from -15dBm to 11dBm. Note that the power of the probe light is measured before the 3dB coupler and the power of the pump light is measured after the coupler. The EAM is reversed bias between 0V~4V. Bandwidth of the BPF is 1 nm. The polarization controllers (PC1 and PC2) are used to set the outputs in TE modes for both probe and pump lights.

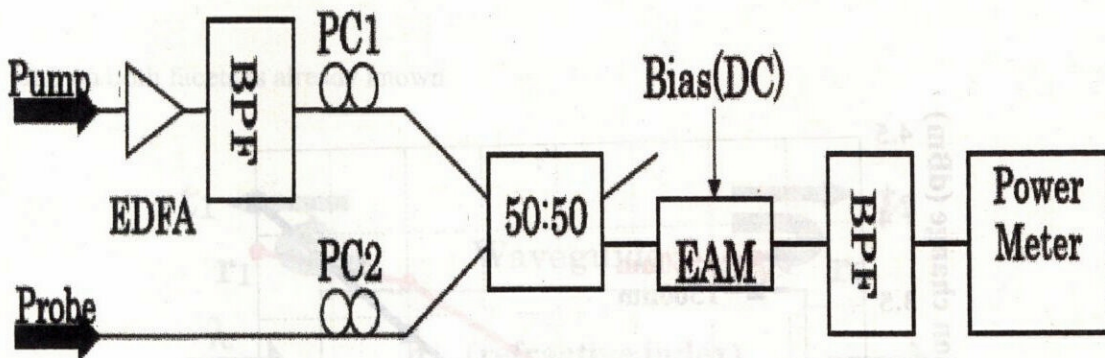


Fig.3.11 Experimental setup for the measurement of cross absorption modulation. EDFA: Er-doped fiber amplifier; PC: polarization controller; BPF: band-pass filter; EAM: electro-absorption modulator.

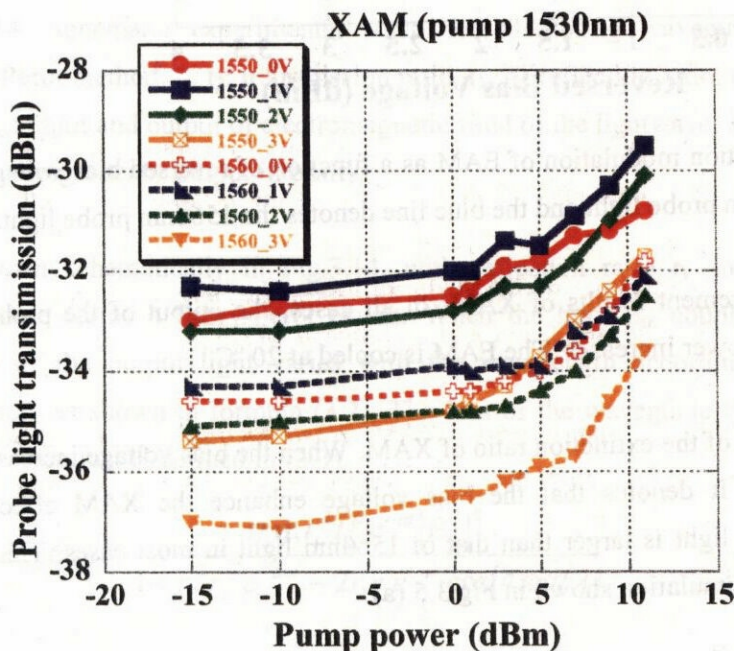


Fig.3.12 Cross absorption modulation results of EAM. The wavelength of the pump light is 1530nm and the powers of the probe light for both 1550nm and 1560nm are 0dBm. The solid lines are for the output of the probe light with 1550nm wavelength and the dotted lines are for those with 1560 nm wavelength.

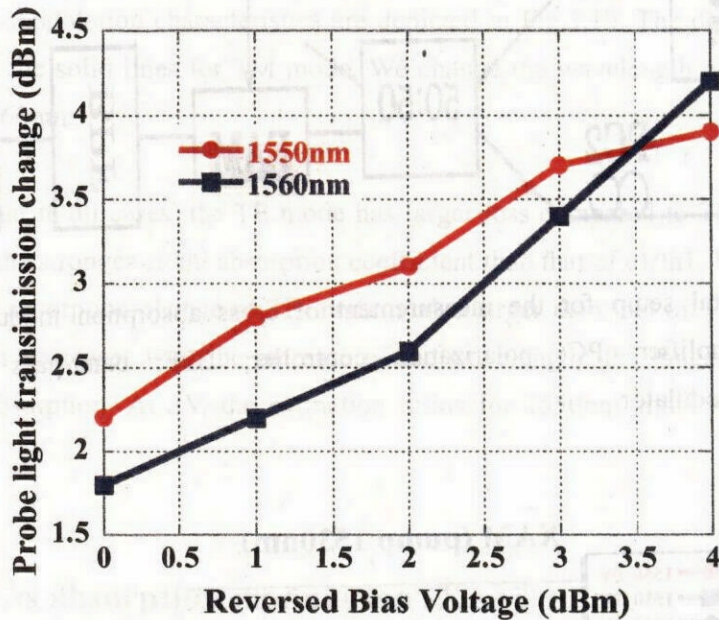


Fig.3.13 Cross absorption modulation of EAM as a function of reversed bias voltage. The red line denotes the 1550nm probe light and the blue line denotes the 1560nm probe light.

Fig.3.12 shows the measurement results of XAM. In all cases, the output of the probe light increases when the pump power increases. The EAM is cooled at 20 °C.

Fig.3.13 shows the changes of the extinction ratio of XAM. When the bias voltage increases, the extinction ratio increases. It denotes that the bias voltage enhance the XAM effect. The extinction ratio of 1550nm light is larger than that of 1560nm light in most cases. This trend matches also well with the simulation shown in Fig.3.5 (a).

3.3.5 Cross phase modulation (XPM)

The cross phase modulation is another important nonlinear in EAM, which is the base of the work in Chapter IV and V. In this subsection , we introduce the Fabry-Perot Etalon method to measure the XPM in EAM

Fabry-Perot Etalon

Fabry-Perot Etalon Method can be used to estimate the loss of a waveguide whose reflection